REPORT DOCUMENTATION PAGE

Form Approved
OMB No. 0704-0188

1. REPORT DATE *(DD-MM-YYYY)*	2. REPORT TYPE	3. DATES COVERED *(From - To)*
03-10-2005	REPRINT	

4. TITLE AND SUBTITLE
A Microchip Ring Trap for Cold Atoms

5a. CONTRACT NUMBER

5b. GRANT NUMBER

5c. PROGRAM ELEMENT NUMBER
62601F

6. AUTHOR(S)
M.B. Crookston[1], P.M. Baker[2] and M.P. Robinson[1]

5d. PROJECT NUMBER
2301

5e. TASK NUMBER
HS

5f. WORK UNIT NUMBER
A1

7. PERFORMING ORGANIZATION NAME(S) AND ADDRESS(ES)

Air Force Research Laboratory
29 Randolph Road
Hanscom AFB, MA 01731-3010

8. PERFORMING ORGANIZATION REPORT NUMBER

9. SPONSORING / MONITORING AGENCY NAME(S) AND ADDRESS(ES)

10. SPONSOR/MONITOR'S ACRONYM(S)
AFRL/VSBYE

11. SPONSOR/MONITOR'S REPORT NUMBER(S)
AFRL-VS-HA-TR-2005-1128

12. DISTRIBUTION / AVAILABILITY STATEMENT
Approved for Public Release; Distribution Unlimited.

[1] Air Force Research Laboratory [2]Tufts University

13. SUPPLEMENTARY NOTES
Reprinted from: Journal of Physics B: Atomic, Molecular and Optical Physics 38 (2005 Institute of Physics Publishing Ltd), Pages 3289 - 3298

14. ABSTRACT

We describe a method to create a circular magnetic waveguide for deBroglie waves on a microchip. The guide is a two-dimensional magnetic minimum for trapping weak-field seeking states of atoms or molecules with a magnetic dipole moment. It is created completely by electric currents in wires that are lithographically patterned on a multi-level chip. We describe the geometry and time-dependent currents of the wires and show that it is possible to wrap the waveguide in a complete circle with minimal perturbations due to the leads or wire crossings. This maximal area geometry is suited for rotation sensing with atom interferometry via the Sagnac effect using either cold thermal atoms and molecules or Bose-condensed systems.

15. SUBJECT TERMS
Cold atoms, inertial force sensors, atom interferometry, microchip, Bose-Einstein condensates

16. SECURITY CLASSIFICATION OF:			17. LIMITATION OF ABSTRACT	18. NUMBER OF PAGES	19a. NAME OF RESPONSIBLE PERSON
a. REPORT	b. ABSTRACT	c. THIS PAGE			Michael Robinson
UNCLAS	UNCLAS	UNCLAS	SAR	10	19b. TELEPHONE NUMBER *(include area code)* 781-377-3595

INSTITUTE OF PHYSICS PUBLISHING JOURNAL OF PHYSICS B: ATOMIC, MOLECULAR AND OPTICAL PHYSICS

J. Phys. B: At. Mol. Opt. Phys. **38** (2005) 3289–3298 doi:10.1088/0953-4075/38/18/001

A microchip ring trap for cold atoms

M B Crookston, P M Baker[1] and M P Robinson

Air Force Research Laboratory, 29 Randolph Road, Hanscom AFB, MA 01731-3010, USA

E-mail: michael.robinson@hanscom.af.mil

Received 21 January 2005, in final form 4 August 2005
Published 5 September 2005
Online at stacks.iop.org/JPhysB/38/3289

Abstract

We describe a method to create a circular magnetic waveguide for deBroglie waves on a microchip. The guide is a two-dimensional magnetic minimum for trapping weak-field seeking states of atoms or molecules with a magnetic dipole moment. It is created completely by electric currents in wires that are lithographically patterned on a multi-level chip. We describe the geometry and time-dependent currents of the wires and show that it is possible to wrap the waveguide in a complete circle with minimal perturbations due to the leads or wire crossings. This maximal area geometry is suited for rotation sensing with atom interferometry via the Sagnac effect using either cold thermal atoms and molecules or Bose-condensed systems.

(Some figures in this article are in colour only in the electronic version)

1. Introduction

The advent of robust cooling and trapping techniques over the last two decades has provided the physics community with large samples of ultra-cold atoms. One relevant application of ultra-cold atoms is that they can make very sensitive atom interferometers, particularly for inertial force sensing [1–3]. What might have once been called the culmination of cooling experiments, the achievement of Bose–Einstein condensation (BEC) has since opened a large number of doors to very innovative experiments [4–7]. Concurrently, microscopic magnetic traps were being explored for use with ultra-cold atoms [8, 9]. Since 2001, microscopic traps have proven to be a greatly simplified way to achieve BEC [10, 11]. Among the several advantages over 'conventional' cooling experiments, these traps are physically small, produce extremely large field gradients/curvatures, require very low power and likely prove versatile in design of atom optics [12–14]. This marriage of cold atoms, atom interferometers and microchips holds the intriguing possibility of an ultra-sensitive inertial force sensor in a small, portable package. Indeed, BECs have already been produced in a portable vacuum system [15].

[1] Tufts University.

0953-4075/05/183289+10$30.00

One of the most promising applications of atom interferometry is the gyroscope. Using the Sagnac effect, the theoretical sensitivity of an atom interferometer bests that of a light interferometer of the same area by a factor of $\frac{mc^2}{\hbar\omega} \sim 10^{11}$ [1]. A proof of concept experiment with a cold caesium beam by Gustavson *et al* showed that cold atom interferometry could exploit the Sagnac effect and compete with state-of-the-art gyroscopes. This experiment used atoms travelling in free space with stimulated Raman transition atom optics. As such, the area enclosed (the Sagnac phase shift is given by $\Delta\Phi = \frac{A \cdot \Omega}{4\pi\lambda v}$) was limited by the small angle between the transverse excitation, which can be several photon recoils from the beam splitter, and the longitudinal velocity of the beam. There have been many ideas put forth to exploit the Sagnac effect using captive atoms or molecules in a ring-shaped trap to maximize this area [16–20]. Another benefit of the circular geometry is that both arms of the interferometer are the same, rejecting some common mode noise. To date, these ring traps, however, have all been achieved with macroscopic fields or permanent magnets. We propose a geometry for producing a ring trap near the surface of a microchip using current-carrying wires produced by photolithography techniques. We also offer a solution for minimizing inhomogeneities introduced by the current leads connecting to the ring. To the best of our knowledge, this is the first proposed microchip ring trap for neutral atoms generated exclusively by electric currents while avoiding these inhomogeneities.

1.1. Two-wire waveguide and ring traps

It is well known that a single wire carrying current and an appropriately applied bias magnetic field produce either an Ioffe–Pritchard or a quadrupole trap in two dimensions, with atoms free along the third dimension [12, 21]. It is also known that a second current-carrying wire parallel to the first can supply the bias field, producing the minimum in the plane of the two wires. We will refer to this 2D wire trap as a two-wire waveguide [22]. Like similar magnetic traps and waveguides for neutral atoms, it uses the interaction between the atom's magnetic moment and the magnetic field governed by the potential $U = -\mu \cdot \boldsymbol{B}$. As Maxwell's equations forbid local maxima in the field, only weak-field seeking states may be trapped (i.e. μ is antiparallel to $\boldsymbol{B}$). By adjusting the strength and direction of the relative currents, one can produce the desired minima either between the wires or outside the wires. Sauer *et al* used this concept to construct a macroscopic ring trap with the minimum between the two guiding wires. In their experiment, they typically ran currents of around 8 A and used a wire separation of 840 μm to produce trap gradients of 1800 G cm^{-1} and frequencies of 590 Hz [16]. Miniaturizing the ring trap is slightly problematic because of the constraints of photolithography and the 2D nature of wire layouts on chips. For example, the leads into the waveguide would necessarily cross, causing major inhomogeneities in the waveguide sufficient to break up the BEC. Nevertheless, using the technique below, it is still possible to design a wire geometry, on chip, to create a circular waveguide while avoiding the inhomogeneities caused by the leads.

2. Four-wire 2D magnetic traps

To avoid the inhomogeneities mentioned above, our design uses two sets of concentric, circular two-wire waveguides as shown in figures 1 and 2. The atoms will be adiabatically switched from one guide to the other at the time when the atoms are farthest from the leads. The waveguide that forms the interferometer is comprised of these overlapping guides. The wires are arranged and the relative currents will be adjusted such that the minimum of the two guides are spatially coincidental over the majority of the ring, see figure 2. Since the guide can be made of the same size and shape over the entire overlap by adjusting the currents, only near

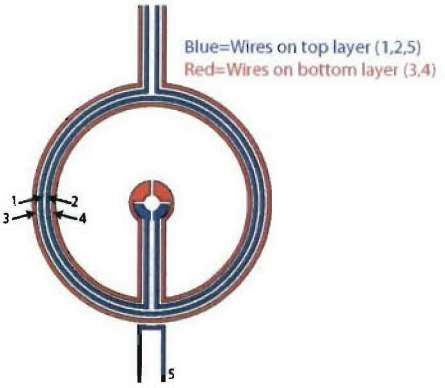

Figure 1. Schematic of the layout of the four wires from above. The two inside wires (2, 4) form one waveguide and the two outside wires (1, 3) form a second waveguide. A wire is passed through the hole in the centre of the chip to create an axial bias field. The wire numbers are referred to in the text.

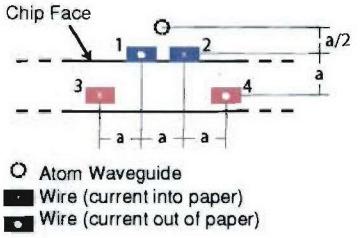

Figure 2. Cross-section of the chip showing a close up of the four wires and the relative direction of the currents. The wire numbers are referred to in the text.

the leads does the potential change. This gives a limit on the spatial extent of any wavepacket, i.e. $\lambda \lesssim r$, where r is the radius of the guide. A non-zero minimum in the ring guide is provided by an azimuthal field produced by an axial wire at the centre of the circle [16, 18]. It is important to note that in the configuration of figure 1 the wires never cross, thereby avoiding any deformations in the guide due to the deposition process.

As an aside, we note that the circular design leads naturally to both quadrupole and Ioffe–Pritchard traps. Quadrupole traps have a zero minimum in the field and vary linearly with small distances from the minimum. Any additional constant bias field serves to shift the zero. Ioffe–Pritchard traps have a non-zero minimum and vary quadratically with small displacements. The non-zero minimum of these traps serve to minimize Majorana 'spin-flip' transitions. These two types of traps are generally formed by U- and Z-shaped wires, respectively, on the chip [12, 23]. The leads going to the circular guides on the chip naturally act to form a modified U-shaped trap (see figure 3). Minimizing Majorana losses is accomplished in one of two ways. The first is the addition of an external wire to form a Z-shaped trap. The second is the addition of an external wire (the lowermost wire, 5, in figure 1) such that a time-averaged orbiting potential (TOP) trap is possible [24, 25]. In either case, the atoms can be trapped and cooled within the ring guide itself. We have chosen the latter case. The current in the leads of the wire trap is then simply ramped down to release the atoms into the guide.

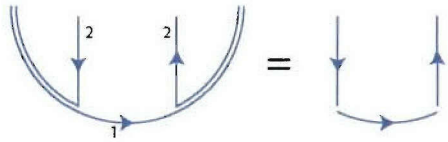

Figure 3. Using the leads and the guide to fashion a 'U trap'

A typical experiment might proceed as follows. A pre-cooled atom cloud is loaded into the U-shaped trap formed by combining the currents of the two upper wires (1, 2), see figure 3. The bias field is supplied by the lower external wire (3). This is the two-dimensional external waveguide pinched off by the leads of the upper internal guide wire. Note that this U-shaped trap may also be used for the initial trapping and cooling, providing an essentially *in situ* solution [26]. As the atoms are trapped and cooled in the guide, there is no need for inefficient transfer of atoms to the guide. The addition of small sinusoidally varying currents to the bottom exterior circular guide wire and an additional external U-shaped wire (5, shown in figure 1) with the appropriate phase creates a time-averaged orbiting potential, or TOP, trap [24, 25] for minimizing Majorana losses. As mentioned above, it is also possible to create a Z-shaped trap if desired.

The 3D trap is turned into a 2D guide (1, 3) simply by ramping down the current in the inner guide leads. Following the recent works of Wang *et al* and Das *et al*, a set of stimulated Rayleigh scattering pulses splits the wavepacket into two coherent packets with momentum $\pm 2\hbar k$ [27, 28]. This is similar to a Bragg scattering process with two outputs [29, 30] and corresponds to a group velocity of 1.2 cm s^{-1} for ^{87}Rb. As the atoms approach $\frac{\pi}{2}$ radians around the circle, the currents in the outer guide (1, 3) are ramped down while the currents in the inner guide (2, 4) are ramped up. By adjusting the currents in the correct way, see section 3, the atoms are transferred from one guide (1, 3) to the other (2, 4). Since the outside wire (1, 3) currents are now off, the atoms continue moving in the waveguide near π radians unaffected by the leads. The packets then travel around the waveguide in this manner any half-integer multiple times and a second set of pulses recombines the wavepackets. After this final set of stimulated Rayleigh scattering pulses, the relative phase shift is measured by counting the relative number of atoms in the 0 versus $\pm 2\hbar k$ momentum states. Through the Sagnac effect, this phase shift is a direct measurement of rotation [1]. We note that a similar scheme can be devised with cold thermal atoms using different hyperfine states that have the same first-order Zeeman shifts (i.e. $F = 2, m_F = 1$ and $F = 1, m_F = -1$) and stimulated Raman transitions [1, 9].

3. Field calculations

We now show that the arrangement described in figures 1 and 2 produce the ring traps as described above. It is instructive to begin with a number of simplifying assumptions to understand the basic idea. More complex and realistic field calculations will then follow.

The following approximations are initially made. The radius of the guide, r, is much larger than the guide's distance, d, to the wires ($r \gg d$). The wires are thin compared with the distance to the atoms ($d \gg l, h$). The magnetic field is everywhere given, in Cartesian coordinates, by equation (1) (i.e. the sum of thin, infinite, straight wires).

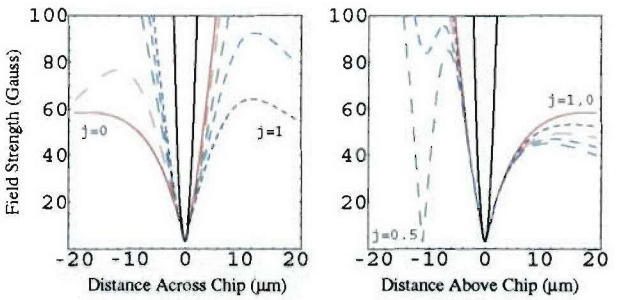

Figure 4. Magnitude of the magnetic field as a function of distance from fixed minimum. The different curves show the transformation from the inside waveguide to the outside waveguide. The harmonic oscillator approximation is the dark line.

$$B(x, y, z) = \{B_x, B_y, B_z\} = \{B_r, B_\theta, B_z\} = \frac{\mu_0 I_b}{2\pi}\left\{0, \frac{1}{r^2 + x^2}, 0\right\} + \sum_{i=1}^{4} \frac{\mu_0 I_i}{2\pi}\left\{-\frac{z - z_i}{(x - x_i)^2 + (z - z_i)^2}, 0, \frac{x - x_i}{(x - x_i)^2 + (z - z_i)^2}\right\}, \tag{1}$$

where each wire has current I_i in the y-direction and the ith wire is at position $(x_i, -, z_i)$. r is the radius of the guide ($r \gg x, y, z$), I_b is the current in an axial wire providing an azimuthal bias field as in section 2 and μ_0 is the permeability of free space. If we make the further simplification that the wires are at positions $\left(-\frac{a}{2}, -, -\frac{a}{2}\right)$, $\left(\frac{a}{2}, -, -\frac{a}{2}\right)$, $\left(-\frac{3a}{2}, -, -\frac{3a}{2}\right)$ and $\left(\frac{3a}{2}, -, -\frac{3a}{2}\right)$, where a is a constant, and the currents are $I_1 = (1 - j)I_0$, $I_2 = -(j)I_0$, $I_3 = -3(1 - j)I_0$ and $I_4 = 3(j)I_0$, the Taylor expansion of the field around the position of the minimum, (0, 0), is then given by equation (2) for $0 \leqslant j \leqslant 1$.

$$\begin{aligned} |B(x, z = 0)| &= \frac{\mu_0 I_b}{2\pi r}\left[1 + \left(\frac{8I_0^2 r^2}{9I_b^2 a^2} - \frac{a^2}{2r^2}\right)\frac{x^2}{a^2} + \left(\frac{64\left(1 - \frac{j}{2}\right)I_0^2 r^2}{27I_b^2 a^2}\right)\frac{x^3}{a^3} + O\left(\frac{x^4}{a^4}\right)\right], \\ |B(x = 0, z)| &= \frac{\mu_0 I_b}{2\pi r}\left[1 + \left(\frac{8I_0^2 r^2}{9I_b^2 a^2} + 0\right)\frac{z^2}{a^2} - \left(\frac{64I_0^2 r^2}{27I_b^2 a^2}\right)\frac{z^3}{a^3} + O\left(\frac{z^4}{a^4}\right)\right]. \end{aligned} \tag{2}$$

Note that the minimum falls along the lines in the xz-plane connecting the two guides. This 2D trap is approximately harmonic and symmetric (for $z, x \ll r, a$) with curvature given by

$$C = \left(\frac{\mathrm{d}^2 B}{\mathrm{d}z^2}\right)_{z=0} = \left(\frac{\mathrm{d}^2 B}{\mathrm{d}x^2}\right)_{x=0} = \frac{8\mu_0 I_0^2 r}{9\pi I_b a^4}.$$

Note that the trap only changes with j at the third-order term in x. The trap frequency then is given in the harmonic oscillator approximation [31] by equation (3).

$$\frac{\omega}{2\pi} = \frac{1}{2\pi}\sqrt{\frac{\mu_B g_F m_F C}{M}} = \frac{1}{2\pi}\sqrt{\frac{8\mu_0 \mu_B g_F m_F}{9\pi M}}\frac{I_0\sqrt{r}}{\sqrt{I_b}a^2}, \tag{3}$$

with μ_B the Bohr magneton, M the mass of the atom and g_F the Landé g-factor. Using ^{87}Rb in the $F = 2, m_F = 2$ state and typical values $r = 1.25$ mm, $a = 15$ μm, $I_b = 2I_0 = 2$ A, this corresponds to $C = 44 \times 10^8$ G cm^{-2} and $\omega = 2\pi \times 84$ kHz. Plots of the field are given in figure 4 with the values of j labelled. One can ramp the current up in one waveguide as the current is ramped down in the other in any fashion, subject to the conditions that it is done

adiabatically and that the sum of the currents remains constant. That is, continuously varying j from 0 to 1. The adiabatic condition is not a stringent one as the field near the minimum is dominated by the constant azimuthal field. For example, one could switch guides very rapidly as the centre of the wavepacket is expected in the centre of the overlap to maximize the extent at which the guides remain homogeneous.

Effectively, we have moved the leads to a distance $\sim\sqrt{2}r$ from the atom cloud, minimizing their impact. To estimate the effect that the leads have on the guide, we note that a good approximation is a circular guide plus a U-shaped wire. The magnetic field due to a U-shaped wire, for the numbers given above and running currents in the guide of 1 A and -3 A, contributes less than 0.1 G to the total field, and more than 99.97% of that is in the z-direction, perpendicular to the chip. That is, these inhomogeneities will be small, varying continuously but slowly, and have the same contribution to atoms on both sides of the circle. Likewise, the energy splitting between trap levels, $\hbar\omega$, with a frequency of 85 kHz, corresponds to 0.06 G. This is of the same order of magnitude as the leads' homogeneous contribution but two orders of magnitude larger than the asymmetric contribution, $\sim$0.001 G, of the leads (the differential effect on opposite sides of the ring). This can be further minimized by moving the leads (i.e. the size of our U-shaped trap) close together, increasing the radius of the circle or increasing the trap frequencies.

Now we must consider the thickness and circular nature of the wires. The finite size of the wires moves the field minimum closer to the chip. This can be compensated for by reducing the currents in the lower circles, i.e. the bias field wires. While these fields are still solvable analytically, due to the complicated nature of the equations we will just state that lowering the maximum current in the bias (bottom) wires from 3 to 2.86 times the current in the guide (top) wires is sufficient to retrieve the symmetry. This is equivalent to lowering the bias field produced by the lower wires to move the field minimum back to the symmetry point compensating for some of the current density being much closer to the atoms.

The circular nature of the guides moves the minimum from the symmetry point as well. This time, the minimum moves towards the centre of the circle. This effect can be compensated for by adjusting the relative currents in both the inner circles. The fields for thin circular wires are given by elliptic integrals as in equation (4) [32, 33].

$$
\begin{aligned}
k^2(r, z, A, R) &= \frac{4Rr}{(R+r)^2 + (z-A)^2}, \\
B_z(r, z) &= \frac{\mu_0 I}{2\pi} \frac{K(k^2) + \frac{R^2 - r^2 - (z-A)^2}{(R-r)^2 + (z-A)^2} E(k^2)}{\sqrt{(R+r)^2 + (z-A)^2}}, \\
B_r(r, z) &= \frac{\mu_0 I}{2\pi} \left(\frac{z-A}{r}\right) \frac{-K(k^2) + \frac{R^2 + r^2 + (z-A)^2}{(R-r)^2 + (z-A)^2} E(k^2)}{\sqrt{(R+r)^2 + (z-A)^2}},
\end{aligned}
\tag{4}
$$

with R the radius of the circle, A the z offset, and E and K the usual complete elliptic integrals. The minimum can be moved back to the symmetry point by adjusting the currents in the following way: $I_1 = 0.96$ A, $I_2 = -1.0$ A, $I_3 = -3.05$ A, $I_4 = 2.84$ A. That is, by increasing the relative strength of the outer guide compared with the inner guide.

Combining both the corrections for the circular wires and the thicknesses of the wires, it is no longer feasible to solve for the fields analytically. Assuming that the wires are 10 μm wide by 5 μm deep, we have done these field calculations by numerically integrating over many (1600) current loops to simulate thick wires and these are shown in figure 5. For reference, we show both contour plots of the magnetic field strength and vector plots of the magnetic field in the same figure. There is no significant difference between the integration done

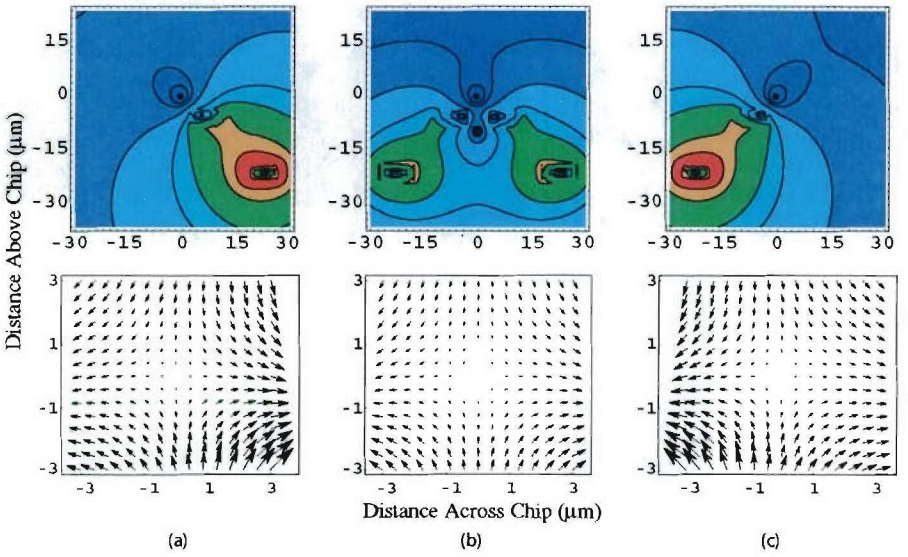

Figure 5. Contour (above) and vector (below) plots of the magnitude of the magnetic field. The quadrupole field minimum is at (0, 0). (a) The field with only the exterior guide energized. (b) The field with both guides energized. (c) The field with only the interior guide energized.

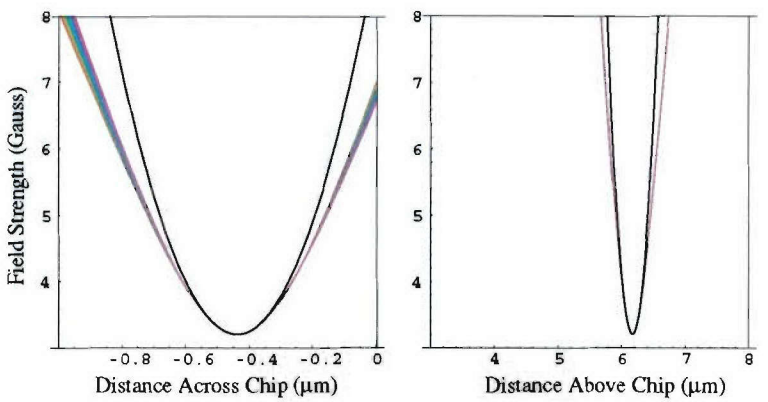

Figure 6. Cross-sections of the magnitude of the magnetic field, full calculation with finite circular wires. The field minimum is offset from the previous ideal minimum by $(-0.44\ \mu\text{m}, -1.33\ \mu\text{m})$.

between running the calculations with 800 and 1600 loops. The minima retain their second-order symmetry with the following currents in place: $I_1 = 0.8439$ A, $I_2 = -0.939$ A, $I_3 = -2.860$ A, $I_4 = 2.860$ A. These corrections also change the strength of the guide. Using the numbers above, the trap curvature becomes $C = 60 \times 10^8$ G cm^{-2} and $\omega = 2\pi \times 98$ kHz. While the actual wires may differ somewhat from the exact geometry stated here, the versatility of the waveguides gives us hope that we can optimize this exchange empirically simply by adjusting the relative currents. In figure 6, we show cross-sections through the minimum of

the field strength produced by thick circular wires. It should be noted that the minimum has moved slightly, across the chip towards the centre by 0.445 μm and closer to the chip by 1.275 μm. The solid black line in figure 6 is a fit, $|B(x, z)| = 3.2 + \frac{C}{2}(x - 6.225)^2 + \frac{C}{2}(z + 0.445)^2$, where x, z are measured in μm and C is 60 G μm^{-2}. Similarly, the trap frequency can be adjusted by changing the relative strengths of the currents. A major issue in manufacturing the chip will be the height of the wires on the chip as well as overlap of the circles. Any misalignment will be directly felt by the positional differences in minima on opposite sides of the ring, which cannot be compensated for by adjusting the currents. The circles, for typical values, will need to be concentric to within a small fraction of the wire widths, typically 100 nm.

We note that the 50 μm^2 cross-section and 3 A maximum current imply a current density of 6×10^9 A m^{-2}, well within the upper limit for gold wires at room temperature (10^{11} A m^{-2}) [22].

4. Practical limits

There are several important practical limits to consider when manipulating cold atoms near the surface of a microchip. Among these are Casimir–Polder forces, Johnson noise, patch potentials and BEC fragmentation [34–37]. In all of these cases, increasing the atom–surface distance mitigates the deleterious effects including atom loss and decoherence. Unfortunately, for a given current density, this also has the affect of decreasing the field gradients and curvature leading to smaller trap frequencies. Many of these effects only become appreciable at exceedingly small atom–surface distances ($\lesssim$1–10 μm) [34]. Currently, however, fragmentation provides perhaps the most stringent limits on the atom–surface distance for BECs, having been observed up to $\sim$100 μm from the wire [35, 37].

We note that any microchip BEC experiment, especially interferometric experiments, must consider fragmentation. There are several methods one might use to deal with fragmentation. The first method is to adjust the atom–surface distance simply by adjusting the wire separation and currents appropriately. One could strike a balance and choose an intermediate distance where fragmentation is manageable. This may or may not require operation in a multimode regime [38]. While this method strives to avoid fragmentation, another strategy is to combat it. Fragmentation does not appear to be a fundamental limitation, but one due to imperfections in the wire (or, rather, unwanted transverse current excitation) [35–37]. It is possible that better lithographic techniques, different materials and other techniques (e.g. using multiple thin 'nano'-wires) will ease the problem.

5. Conclusion

We have proposed a ring trap design produced by current-carrying wires on a microchip that minimizes the inhomogeneities caused by the leads to the ring. The trap frequencies can be as large as MHz for single-mode operation, produced entirely by electric currents. This design leads naturally to a Sagnac interferometer for either cold thermal atoms or Bose–Einstein condensates. Currently, our design encloses an area of 4.9 mm^2, with a baseline (diameter) of 2.5 mm, and is scalable. Likewise, with such large trap frequencies available, it is possible that this could approach the low density, strongly interacting (hard core) regime [28, 39–41]. It has been shown that high visibility interference fringes of this Tonks gas on a ring are theoretically possible [28]. This design provides a means for atom interferometry on a microchip while

reducing common mode noise, provides *in situ* loading and avoids some of the problems associated with miniaturizing ring traps.

Acknowledgments

The authors gratefully acknowledge the generous support from the Air Force Office of Scientific Research (AFOSR) and the Defense Advanced Research Projects Agency (DARPA). PB would like to thank Tufts University and the Air Force PALACE Acquire program. The authors gratefully acknowledge useful conversations with Jim Gillespie at AFRL/SNDD for his insight into chip manufacturing.

References

[1] Gustavson T L, Bouyer P and Kasevich M A 1997 *Phys. Rev. Lett.* **78** 2046
[2] Kasevich M and Chu S 1991 *Phys. Rev. Lett.* **67** 181
[3] Hinds E A, Vale C J and Boshier M G 2001 *Phys. Rev. Lett.* **86** 1462
[4] Roberts J L, Claussen N R, Cornish S L, Donley E A, Cornell E A and Wieman C E 2001 *Phys. Rev. Lett.* **86** 4211
[5] Dürr S, Volz T, Marte A and Rempe G 2004 *Phys. Rev. Lett.* **92** 020406
[6] Regal C A, Greiner M and Jin D S 2004 *Phys. Rev. Lett.* **92** 040403
[7] Inouye S, Pfau T, Gupta S, Chikkatur A P, Görlitz A, Pritchard D E and Ketterle W 1999 *Nature* **402** 641
[8] Weinstein J D and Libbrecht K G 1995 *Phys. Rev.* A **52** 4004
[9] Treutlein P, Hommelhoff P, Steinmetz T, Hänsch T W and Reichel J 2004 *Phys. Rev. Lett.* **92** 203005
[10] Ott H, Fortagh J, Schlotterbeck G, Grossmann A and Zimmermann C 2001 *Phys. Rev. Lett.* **87** 230401
[11] Hänsel W, Hommelhoff P, Hänsch T W and Reichel J 2001 *Nature* **413** 498
[12] Reichel J, Hänsel W and Hänsch T W 1999 *Phys. Rev. Lett.* **83** 3398
[13] Lev B 2003 *Quantum Inform. Comput.* **3** 450–64
[14] Dekker N H, Lee C S, Lorent V, Thywissen J H, Smith S P, Drndić M, Westervelt R M and Prentiss M 2000 *Phys. Rev. Lett.* **84** 1124
[15] Du S, Squires M B, Imai Y, Czaia L, Saravanan R A, Bright V, Reichel J, Hänsch T W and Anderson D Z 2004 *Phys. Rev.* A **70** 053606
[16] Sauer J A, Barrett M D and Chapman M S 2001 *Phys. Rev. Lett.* **87** 270401
[17] Wu S, Rooijakkers W, Striehl P and Prentiss M 2004 *Phys. Rev.* A 70 013409
[18] Arnold A S and Riis E 2002 *J. Mod. Opt.* **49** 959
[19] Katz D P 1997 *J. Chem. Phys.* **107** 8491
[20] Thompson D, Lovelace R V E and Lee D M 1989 *J. Opt. Soc. Am.* B 6 2227
[21] Denschlag J, Cassettari D and Schmiedmayer J 1999 *Phys. Rev. Lett.* **82** 2014
[22] Reichel J 2002 *Appl. Phys.* B **75** 469–87
[23] Haase A, Cassettari D, Hessmo B and Schmiedmayer J 2001 *Phys. Rev.* A **64** 043405
[24] Petrich W, Anderson M H, Ensher J R and Cornell E A 1995 *Phys. Rev. Lett.* **74** 3352
[25] Arnold A S 2004 *J. Phys. B: At. Mol. Opt. Phys.* **37** L29
[26] Vengalattore M, Rooijakkers W and Prentiss M 2002 *Phys. Rev.* A **66** 053403
[27] Wang Y, Anderson D Z, Bright V M, Cornell E A, Diot Q, Kishimoto T, Prentiss M, Saravanan R A, Segal S and Wu S 2005 *Phys. Rev. Lett.* **94** 090405
[28] Das K K, Girardeau M D and Wright E M 2002 *Phys. Rev. Lett.* **89** 170404
[29] Stenger J, Inouye S, Chikkatur A P, Stamper-Kurn D M, Pritchard D E and Ketterle W 1999 *Phys. Rev. Lett.* **82** 4569
[30] Kozuma M, Deng L, Hagley E W, Wen J, Lutwak R, Helmerson K, Rolston S L and Phillips W D 1999 *Phys. Rev. Lett.* **82** 871
[31] Folman R, Krüger P, Schmiedmayer J, Denschlag J and Henkel C 2002 *Adv. At. Mol. Opt. Phys.* **48** 263–355
[32] Bergeman T, Erez G and Metcalf H J 1987 *Phys. Rev.* A **35** 1535
[33] Smythe W R 1989 *Static and Dynamic Electricity* (London: Taylor and Francis)
[34] Lin Y, Teper I, Chin C and Vuletic V 2004 *Phys. Rev. Lett.* **92** 050404
[35] Estéve J, Aussibal C, Schumm T, Figl C, Mailly D, Bouchoule I, Westbrook C I and Aspect A 2004 *Phys. Rev.* A **70** 043629

[36] Krafi S, Günther A, Ott H, Wharam D, Zimmerman C and Fortágh J 2002 *J. Phys. B: At. Mol. Opt. Phys.* **35** L469
[37] Leanhardt A E, Chikkatur A P, Kielpinski D, Shin Y, Gustavson T L, Ketterle W and Pritchard D E 2002 *Phys. Rev. Lett.* **89** 040401
[38] Andersson E, Calarco T, Folman R, Andersson M, Hessmo B and Schmiedmayer J 2002 *Phys. Rev. Lett.* **99** 100401
[39] Ketterle W and van Druten N J 1996 *Phys. Rev.* A **54** 656
[40] Olshanii M 1998 *Phys. Rev. Lett.* **81** 938
[41] Petrov D S, Shlyapnikov G V and Walraven J T M 2000 *Phys. Rev Lett.* **85** 3745